ORIGINAL PAPER

Hassan M. Badawi · Wolfgang Förner ·
Khalid S. Al-Ghamdi

Conformational stability and normal coordinate analyses for 1-halovinyl azides CH$_2$=CX–NNN (X is F, Cl and Br)

Abstract The conformational behavior of 1-halovinyl azides CH$_2$=CX–NNN (X=F, Cl and Br) were investigated by DFT-B3LYP and ab initio MP2 calculations with the 6-311++G** basis set. The molecules were predicted to exist predominantly in the *trans* (the vinyl CH$_2$=CH– and the azide –NNN groups are *trans* to each other) conformation. The relative energy between *cis* and *trans* were calculated to decrease in order: bromide>chloride>fluoride. Full optimization was performed at the ground and transition states in the molecule at both MP2 and B3LYP levels. The barrier to internal rotation around the C–N single bond in the three molecules was calculated to be about 4–5 kcal mol^{-1}. The vibrational frequencies were computed at the DFT-B3LYP level and the calculated infrared and Raman spectra of the *cis–trans* mixture of the three molecules were plotted. Complete vibrational assignments were made on the basis of normal coordinate calculations for both stable conformers of the three molecules.

Keywords Ab initio calculations · Structural stability · Vibrational spectra and assignments · Rotational barrier · 1-Fluorovinyl azide · 1-Chlorovinyl azide · 1-Bromovinyl azide

Introduction

Recently the structural and conformational stability of some vinyl compounds of the general formula CH$_2$=CH–M=X=Y (–MXY is –NCO, –NNN, –CHCO or –NHCN) were investigated by DFT-B3LYP calculations [1, 2, 3, 4]. When –MXY was isocyanate –NCO and ketene –CHCO, [1] azide –NNN [2] and cyanamide –NHCN, [3] all the molecules were predicted to exist in the planar

cis⇔*trans* conformational equilibrium with the non-planar *gauche* conformations being transition states.

The stability of the molecules only in the planar structure was explained as a result of pronounced conjugation effects. Furthermore, the size of the rotational barrier in these molecules was found to be significantly dependent on the type of the substituent. In vinyl ketene CH$_2$=CH–CHCO [1] and vinyl cyanamide CH$_2$=CH–NHCN [3] the rotational barrier was calculated to be about 7 kcal mol^{-1}, while that in the corresponding isocyanate CH$_2$=CH–NCO is about 2 kcal mol^{-1}. For vinyl azide, [2] the *cis* and the *trans* conformers were predicted to have comparable relative stabilities with a rotational barrier of the order of 5 kcal mol^{-1}. [2] However, an earlier microwave study of vinyl azide showed that the *cis* conformation is slightly more stable than the *trans*. [4]

In the present study, we investigated the effect of halogen substitution (F, Cl and Br) on the conformational stability of vinyl azide. The energies of the three halogenated vinyl azide molecules in their possible structures were optimized at the DFT-B3LYP/6-311++G** level and the structural parameters optimized at both MP2 and B3LYP levels. The vibrational frequencies were computed and the zero-point corrections were included in the calculation of the energies of ground and transition states. Also, normal coordinate analyses were carried out and the potential energy distributions (PED) among symmetry coordinates for the stable conformers of the molecule were calculated. The vibrational assignments of the normal modes were made based on the calculated PED values and the results are presented here.

Ab initio calculations

The Gaussian 98 program, [5] running on an IBM RS/6000 43P model 260 workstation, was used to carry out the DFT-B3LYP calculations. The 6-311++G** basis set was employed to optimize the structures and predict the energies and dipole moments of halovinyl azides 1-CH$_2$=CX–NNN (where X= F, Cl and Br) in their stable

H. M. Badawi (✉) · W. Förner · K. S. Al-Ghamdi
Department of Chemistry,
King Fahd University of Petroleum and Minerals,
31261 Dhahran, Saudi Arabia
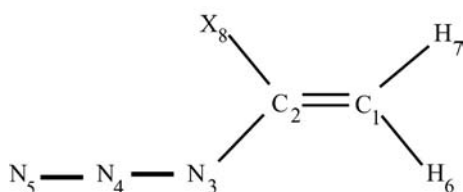e-mail: hbadawi@kfupm.edu.sa

Fig. 1 Atom numbering for 1-halovinyl azides (X=F, Cl and Br) in the *trans* conformations

conformations (Fig. 1). The optimized energies and structural parameters of the three molecules in the two conformations are shown in Tables 1, 2 and 3.

Asymmetric torsional potential function

The potential scan for the internal rotation about the C–N single bond in the three molecules was obtained by

Table 1 Calculated structural parameters, total dipole moment and rotational constants (MHz) at DFT-B3LYP/6-311++G** level for the *cis* and *trans* conformations of 1-fluorovinyl (X=F), 1-chlorovinyl (X=Cl) and 1-bromovinyl (X=Br) azides

Parameter	Fluoride		Chloride		Bromide	
	Cis	*Trans*	*Cis*	*Trans*	*Cis*	*Trans*
Bond length (Å)						
$r(C_1=C_2)$	1.329	1.327	1.333	1.331	1.333	1.331
$r(C_2–N_3)$	1.401	1.394	1.408	1.399	1.407	1.399
$r(N_3–N_4)$	1.235	1.237	1.236	1.234	1.237	1.233
$r(N_4–N_5)$	1.129	1.130	1.130	1.131	1.130	1.131
$r(C_1–H_6)$	1.081	1.079	1.083	1.082	1.084	1.083
$r(C_1–H_7)$	1.080	1.080	1.079	1.079	1.079	1.079
$r(C_2–X_8)$	1.339	1.354	1.745	1.765	1.906	1.929
Bond angle (degree)						
$(C_1C_2N_3)$	130.2	124.4	128.0	121.4	128.1	121.3
$(C_2N_3N_4)$	117.4	118.3	117.2	120.4	117.3	121.1
$(N_3N_4N_5)$	187.0	187.9	187.1	188.1	187.3	188.2
$(C_2C_1H_6)$	121.2	119.8	121.0	119.3	120.8	119.2
$(C_2C_1H_7)$	119.7	120.0	120.7	121.2	121.1	121.5
$(C_1C_2X_8)$	121.6	121.4	122.0	121.2	121.8	120.7
$(C_1C_2N_3N_4)$	0.0	180.0	0.0	180.0	0.0	180.0
Dipole moment (debye)						
μ_t	1.50	1.22	1.39	1.29	1.33	1.27
Rotational constants (MHz)						
A	10,235	10,495	8,856	4,993	8,258	3,502
B	2,445	2,590	1,646	2,387	1,098	1,900
C	1,974	2,077	1,388	1,615	969	1,232

Table 2 Calculated structural parameters, total dipole moment and rotational constants (MHz) at MP2/6-311++G** level for the *cis* and *trans* conformations of 1-fluorovinyl (X=F), 1-chlorovinyl (X=Cl) and 1-bromovinyl (X=Br) azides

Parameter	Fluoride		Chloride		Bromide	
	Cis	*Trans*	*Cis*	*Trans*	*Cis*	*Trans*
Bond length (Å)						
$r(C_1=C_2)$	1.338	1.335	1.344	1.341	1.345	1.343
$r(C_2–N_3)$	1.404	1.399	1.413	1.407	1.413	1.406
$r(N_3–N_4)$	1.241	1.245	1.243	1.243	1.243	1.242
$r(N_4–N_5)$	1.153	1.150	1.153	1.151	1.154	1.152
$r(C_1–H_6)$	1.082	1.080	1.085	1.083	1.086	1.084
$r(C_1–H_7)$	1.081	1.081	1.081	1.081	1.081	1.081
$r(C_2–X_8)$	1.332	1.348	1.721	1.738	1.883	1.903
Bond angle (degree)						
$(C_1C_2N_3)$	129.3	123.8	126.8	120.5	126.8	120.3
$(C_2N_3N_4)$	115.5	116.7	115.4	118.5	115.3	119.3
$(N_3N_4N_5)$	187.1	188.1	187.0	188.4	187.1	188.5
$(C_2C_1H_6)$	120.6	119.2	120.7	119.1	120.5	118.9
$(C_2C_1H_7)$	119.4	119.7	120.2	120.5	120.5	120.9
$(C_1C_2X_8)$	122.2	121.8	122.9	122.0	122.6	121.5
$(C_1C_2N_3N_4)$	0.0	180.0	0.0	180.0	0.0	180.0
Dipole moment (debye)						
μ_t	1.97	0.74	1.75	0.91	1.71	0.95
Rotational constants (MHz)						
A	10,188	10,469	8,974	5,035	8,425	3,479
B	2,455	2,585	1,654	2,406	1,102	1,940
C	1,978	2,073	1,397	1,628	974	1,246

Table 3 Computed total energies (Hartrees), relative energies and rotational barriers (kcal mol^{-1}) at B3LYP/6-311++G** level of calculations in 1-fluoro, 1-chloro and 1-bromovinyl azide

	Fluoride		
	Cis	*Trans*	TS
Total energy (B3LYP)	−341.51667	−341.51831	−341.51121
Relative energy		1.029	
Cis–trans barrier		3.426	
Trans–cis barrier		4.455	
Zero-point correction	0.04731	0.04717	0.04707
Corrected total energy	−341.46937	−341.47113	−341.46414
Corrected relative energy		1.104	
Corrected *cis–trans* barrier		3.28188	
Corrected *trans–cis* barrier		4.38629	
	Chloride		
	Cis	*Trans*	TS
Total energy (B3LYP)	−701.86696	−701.86986	−701.86313
Relative energy		1.819	
Cis–trans barrier		2.403	
Trans–cis barrier		4.223	
Zero-point correction	0.04574	0.04572	0.045616
Corrected total energy	−701.82122	−701.82414	−701.81751
Corrected relative energy		1.832	
Corrected *cis–trans* barrier		2.32806	
Corrected *trans–cis* barrier		4.16039	
	Bromide		
	Cis	*Trans*	TS
Total energy (B3LYP)	−2815.78622	−2815.78967	−2815.78329
Relative energy		2.165	
Cis–trans barrier		1.839	
Trans–cis barrier		4.004	
Zero-point correction	0.04505	0.04507	0.04499
Corrected total energy	−2815.74117	−2815.74460	−2815.73829
Corrected relative energy		2.152	
Corrected *cis–trans* barrier		1.80722	
Corrected *trans–cis* barrier		3.95959	

Table 4 Calculated potential constants (kcal mol^{-1}) for the asymmetric torsion in 1-halovinyl azides at B3LYP/6-311++G** level

Potential constants[a]	Fluorovinyl azide	Chlorovinyl azide	Bromoviny azide
V_0	1.025	1.823	2.501
V_1	−1.452	−2.334	1.341
V_2	3.942	3.306	−1.452
V_3	0.448	0.519	−0.265
V_4	−0.048	−0.073	0.045
V_5	−0.021	−0.005	0.011
V_6	−0.303	0.007	−0.008

[a]E_0 is −341.518307, −701.869865, −2815.789673 hartrees for the fluoride, chloride and bromide, respectively

allowing the CCNN dihedral angle (φ) in the three molecules to vary from 0° (*cis* position) to 180° (*trans* position). Full geometry optimizations at each of the fixed dihedral angles (φ) of 15°, 30°, 45°, 60°, 75°, 90°, 105°, 120°, 135°, 150°, and 165° were carried out for the three molecules. The computed relative energies and barriers to interconversion at the MP2/6-311++G** and the DFT-B3LYP/6-311++G** levels of calculations are listed in Tables 3 and 4. Also, the zero-point corrections, the corrected relative energies and the corrected energy barriers in this series of molecules were computed at the DFT-B3LYP/6-311++G** level and are shown in Table 3. The torsional potential was represented as a Fourier cosine series in the dihedral angle (φ):

$$E(\varphi) = E_0 + V_0 + \sum_{n=1}^{n=6} (V_n/2)[1 - \cos(n\varphi)]$$

where the potential coefficients from V_1 to V_6 are considered adequate to describe the potential function. The results of the energy optimizations at the B3LYP level were used to calculate the six coefficients by least-squares fitting for the three systems (Table 4). The potential functions of 1-halovinyl azides are shown in Fig. 2.
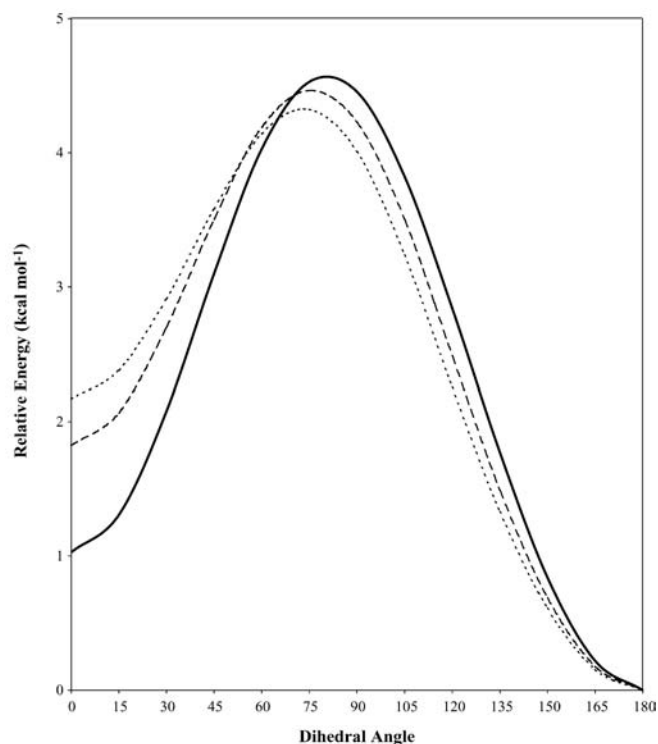
Fig. 2 Potential surface scan for the asymmetric torsion in 1-fluorovinyl azide (solid line), 1-chlorovinyl azide (dashed line) and 1-bromovinyl azide (dotted line)

Vibrational frequencies and normal coordinate analyses

The optimized structural parameters of the three molecules were used to compute the vibrational frequencies at the DFT-B3LYP/6-311++G** level of calculation. 1-Halovinyl azides in their planar *cis* and *trans* conformations have C_s symmetry. In 1-halovinylazides, the 18 vibrational modes span the irreducible representations: 13 A' and 5 A'. The A' modes should be polarized whereas the A" modes should be depolarized in the Raman spectra of the liquid.

Normal coordinate analyses were carried out for the stable *cis* and *trans* conformers of the molecules to provide a complete assignment of the fundamental vibrational frequencies. A computer program was written for this purpose by following Wilson's method. [6] The Cartesian coordinates for the stable conformers together with the normal modes (in Cartesian coordinates) and the frequencies from Gaussian 98 output were used as an input in the program. A complete set of internal coordinates (Table 5) was used to form symmetry coordinates (Table 6) in the molecular systems. The potential energy distribution (PED) for each normal mode among the symmetry coordinates was calculated and is given in Tables 7, 8, 9, 10, 11, 12.

A complete vibrational assignment of the fundamentals was proposed. The assignments were made based on calculated PED, infrared band intensities, Raman line

Table 5 Internal coordinate definitions (for atom denotation see Fig. 1) for 1-fluorovinyl (X=F), 1-chlorovinyl (X=Cl) and 1-bromovinyl (X=Br) azides

No.	Coordinate		Definition
1	C_1–C_2	Stretch	R
2	C_2–N_3	Stretch	X
3	N_3–N_4	Stretch	S
4	N_4–N_5	Stretch	Q
5	C_1–H_6	Stretch	P_1
6	C_1–H_7	Stretch	P_2
7	C_2–X_8	Stretch	T
8	$C_1C_2N_3$	Bend	β_1
9	$N_3C_2X_8$	Bend	β_2
10	$C_1C_2X_8$	Bend	β_3
11	$C_2N_3N_4$	Bend	γ
12	$N_3N_4N_5$	Bend	σ
13	$H_6C_1H_7$	Bend	α_1
14	$C_2C_1H_6$	Bend	α_2
15	$C_2C_1H_7$	Bend	α_3
16	$C_2N_3N_4N_5$	Wag	χ
17	$X_8C_2C_1H_7$	Torsion (out of plane)	ω
18	$(H_6C_1C_2N_3{-}H_7C_1C_2N_3)$	Torsion	ξ_1
19	$(H_6C_1C_2N_3{+}H_7C_1C_2N_3)$	Torsion	ξ_2
20	$C_1C_2N_3N_4$ $X_8C_2N_3N_4$	Asymmetric torsion	τ

Table 6 Symmetry coordinates for 1-halovinyl azides

Species	Description	Symmetry coordinate[a]
A'		
CH_2	Antisymmetric stretch	$S_1=P_1-P_2$
CH_2	Symmetric stretch	$S_2=P_1+P_2$
C_2–X_8	Stretch	$S_3=T$
NNN	Antisymmetric stretch	$S_4=S-Q$
C=C	Stretch	$S_5=R$
C–N	Stretch	$S_6=X$
NNN	Symmetric stretch	$S_7=S+Q$
CH_2	Deformation	$S_8=2\alpha_1-\alpha_2-\alpha_3$
CH_2	Wag	$S_9=\alpha_2-\alpha_3$
C_2–X_8	In-plane bend	$S_{10}=\beta_2-\beta_3$
NNN	In-plane bend	$S_{11}=\sigma$
C=C–N	In-plane bend	$S_{12}=2\beta_1-\beta_2-\beta_3$
CNN	In-plane bend	$S_{13}=\gamma$
A"		
C_2–X_8	Torsion (out of plane)	$S_{14}=\omega$
CH_2	Deformation I	$S_{15}=\xi_1$
CH_2	Deformation II	$S_{16}=\xi_2$
NNN	Wag (out-of-plane bend)	$S_{17}=\chi$
Asymmetric torsion		$S_{18}=\tau$

activities, depolarization ratios and comparison with experimental values for similar molecules. The data of the vibrational assignments are listed in Tables 7, 8, 9, 10, 11, 12.

The vibrational infrared and Raman spectra were calculated using the computational method described previously. [7, 8] To calculate the Raman spectra, the frequencies v_j, the scattering activities S_j, and the depolarization ratios ρ_j were obtained from the DFT-B3LYP/ 6-311++G** calculations. The calculated vibrational infrared and Raman spectra of the 1-fluorovinyl

Table 7 Calculated vibrational frequencies (cm^{-1}) at B3LYP/6-311++G** level for the *cis* conformer of 1-fluorovinyl azide

Sym.	No.	Freq.	IR int.[a]	Raman activity	Depol. ratio	PED
A'	v_1	3,274	0.1	55.8	0.6	100%S_1 (CH$_2$ anti-sym. str.)
	v_2	3,178	4.9	78.0	0.1	99%S_2 (CH$_2$ sym. str.)
	v_3	2,269	546.8	46.0	0.5	92%S_4 (NNN anti.sym. str.)
	v_4	1,698	206.2	116.1	0.1	72%S_5 (C=C str.)
	v_5	1,423	35.8	31.4	0.2	80%S_8 (CH$_2$ deform.)
	v_6	1,367	334.4	20.4	0.4	46%S_7 (NNN sym. str.), 20%S_6 (C–N str.)
	v_7	1,235	116.9	5.9	0.7	31%S_3 (C$_2$–F$_8$ str.), 24%S_7 (NNN sym. str.), 23%S_9 (CH$_2$ wag)
	v_8	958	30.5	3.7	0.2	57%S_9 (CH$_2$ wag), 35%S_3 (C$_2$–F$_8$ str.)
	v_9	894	40.5	9.5	0.3	41%S_6 (C–N str.), 15%S_5 (C=C str.)
	v_{10}	641	12.5	4.9	0.2	45%S_{11} (NNN in-plane bend), 30%S_{13} (CNN in-plane bend)
	v_{11}	476	0.2	3.7	0.7	62%S_{10} (C$_2$–F$_8$ in-plane bend), 16%S_{12} (C=C–N in-plane bend)
	v_{12}	449	4.2	0.4	0.3	50%S_{12} (C=C–N in-plane bend), 21%S_{10} (C$_2$–F$_8$ in-plane bend), 16%S_{11} (NNN in-plane bend),10%S_9 (CH$_2$ wag)
	v_{13}	173	1.7	12.3	0.6	59%S_{13} (CNN in-plane bend), 25%S_{11} (NNN in-plane bend), 16%S_{12} (C=C–N in-plane bend).
A''	v_{14}	817	77.5	5.1	0.8	94%S_{15} (CH$_2$ deform. I)
	v_{15}	693	0.0	0.0	0.8	77%S_{14} (C$_2$–F$_8$ out-of-plane bend), 19%S_{16} (CH$_2$ deform. II)
	v_{16}	608	0.0	1.8	0.8	79%S_{16} (CH$_2$ deform. II), 18%S_{14} (C$_2$–F$_8$ out-of-plane bend)
	v_{17}	521	8.1	0.8	0.8	96%S_{17} (NNN wag)
	v_{18}	90	0.0	2.7	0.8	98%S_{18} (NNN asym. torsion)

[a] IR intensities and Raman activities are calculated in km mol^{-1} and Å^4 amu^{-1} respectively

Table 8 Calculated vibrational frequencies (cm^{-1}) at B3LYP/6-311++G** level for the *trans* conformer of 1-fluorovinyl azide

Sym.	No.	Freq.	IR int.[a]	Raman activity	Depol. ratio	PED
A'	v_1	3,290	0.2	63.2	0.7	100%S_1 (CH$_2$ antisym. str.)
	v_2	3,189	8.5	98.3	0.1	99%S_2 (CH$_2$ sym. str.)
	v_3	2,270	783.0	68.8	0.4	92%S_4 (NNN antisym. str.)
	v_4	1,715	307.6	255.6	0.2	74%S_5 (C=C str.)
	v_5	1,414	64.0	113.4	0.3	67%S_8 (CH$_2$ deform.), 14%S_6 (C–N str.), 14%S_7 (NNN sym. str.)
	v_6	1,368	119.0	31.2	0.3	42%S_7 (NNN sym. str.), 23%S_8 (CH$_2$ deform.), 16%S_6 (C–N str.)
	v_7	1,211	120.0	2.6	0.7	29%S_9 (CH$_2$ wag), 22%S_7 (NNN sym. str.), 22%S_3 (C$_2$–F$_8$ str.), 15%S_{12} (C=C–N in-plane bend)
	v_8	931	44.9	5.7	0.2	51%S_9 (CH$_2$ wag), 36%S_3 (C$_2$–F$_8$ str.)
	v_9	863	4.2	4.0	0.4	37%S_6 (C–N str.), 30%S_3 (C$_2$–F$_8$ str.)
	v_{10}	692	22.5	14.9	0.3	29%S_{13} (CNN in-plane bend), 28%S_{11} (NNN in-plane bend), 22%S_{10} (C$_2$–F$_8$ in-plane bend)
	v_{11}	479	3.5	2.8	0.6	50%S_{10} (C$_2$–F$_8$ in-plane bend), 38%S_{11} (NNN in-plane bend)
	v_{12}	413	1.4	6.2	0.5	66%S_{12} (C=C–N in-plane bend), 12%S_9 (CH$_2$ wag), 12%S_{10} (C$_2$–F$_8$ in-plane bend)
	v_{13}	172	0.1	3.5	0.5	60%S_{13} (CNN in-plane bend), 23%S_{11} (NNN in-plane bend), 12%S_{12} (C=C–N in-plane bend)
A''	v_{14}	837	75.9	9.9	0.8	97%S_{15} (CH$_2$ deform. I)
	v_{15}	710	0.4	0.3	0.8	77%S_{14} (C$_2$–F$_8$ out-of-plane bend), 23%S_{16} (CH$_2$ deform. II)
	v_{16}	598	1.0	2.5	0.8	68%S_{16} (CH$_2$ deform. II), 19%S_{14} (C$_2$–F$_8$ out-of-plane bend)
	v_{17}	484	4.9	0.1	0.8	93%S_{17} (NNN wag)
	v_{18}	72	1.4	0.2	0.8	100%S_{18} (NNN asym. torsion).

[a] IR intensities and Raman activities are calculated in km mol^{-1} and Å^4 amu^{-1} respectively

Table 9 Calculated vibrational frequencies (cm^{-1}) at B3LYP/6-311++G** level for the *cis* conformer of 1-chlorovinyl azide

Sym.	No.	Freq.	IR int.[a]	Raman activity	Depol. ratio	PED
A'	ν_1	3,264	0.3	61.0	0.6	95%S_1 (CH$_2$ antisym. str.)
	ν_2	3,161	3.5	76.3	0.1	94%S_2 (CH$_2$ sym. str.)
	ν_3	2,254	531.1	53.5	0.5	91%S_4 (NNN antisym. str.)
	ν_4	1,648	121.5	86.9	0.1	74%S_5 (C=C str.), 15%S_8 (CH$_2$ deform.)
	ν_5	1,424	27.5	40.3	0.2	79%S_8 (CH$_2$ deform.)
	ν_6	1,328	268.3	24.7	0.4	61%S_7 (NNN sym. str.), 16%S_6 (C–N str.)
	ν_7	1,144	117.1	3.7	0.7	55%S_9 (CH$_2$ wag), 13%S_7 (NNN sym. str.),
	ν_8	914	17.4	7.2	0.6	52%S_6 (C–N str.), 21%S_9 (CH$_2$ wag), 10%S_7 (NNN sym. str.),
	ν_9	772	86.0	3.2	0.2	33%S_3 (C$_2$–Cl$_8$ str.), 25%S_{13} (CNN in-plane bend), 16%S_9 (CH$_2$ wag), 14%S_{11} (NNN in-plane bend)
	ν_{10}	581	5.4	8.7	0.1	44%S_{11} (NNN in-plane bend), 28%S_3 (C$_2$–Cl$_8$ str.), 12%S_{13}
	ν_{11}	422	2.7	2.3	0.5	62%S_{12} (C=C–N in-plane bend), 18%S_3 (C$_2$–Cl$_8$ str.)
	ν_{12}	341	0.4	4.8	0.7	79%S_{10} (C$_2$–Cl$_8$ in-plane bend)
	ν_{13}	166	1.0	9.4	0.5	54%S_{13} (CNN in-plane bend),28%S_{11} (NNN in-plane bend), 16%S_{12} (C=C–N in-plane bend).
A"	ν_{14}	845	60.3	4.4	0.8	96%S_{15} (CH$_2$ deform. I)
	ν_{15}	680	0.2	0.3	0.8	69%S_{16} (CH$_2$ deform. II), 30%S_{14} (C$_2$–Cl$_8$ out-of-plane bend)
	ν_{16}	535	10.1	1.2	0.8	60%S_{17} (NNN wag), 23%S_{14} (C$_2$–Cl$_8$ out-of-plane bend), 14%S_{16} (CH$_2$ deform. II)
	ν_{17}	526	0.4	0.5	0.8	46%S_{14} (C$_2$–Cl$_8$ out-of-plane bend), 37%S_{17} (NNN wag), 15%S_{16} (CH$_2$ deform. II)
	ν_{18}	75	0.0	2.5	0.8	98%S_{18} (NNN asym. torsion)

[a] IR intensities and Raman activities are calculated in km mol^{-1} and Å^4 amu^{-1} respectively

Table 10 Calculated vibrational frequencies (cm^{-1}) at B3LYP/6-311++G** level for the *trans* conformer of 1-chlorovinyl azide

Sym.	No.	Freq.	IR int.[a]	Raman activity	Depol. ratio	PED
A'	ν_1	3,278	0.5	72.2	0.7	98%S_1 (CH$_2$ antisym. str.)
	ν_2	3,174	4.4	117.2	0.1	97%S_2 (CH$_2$ sym. str.)
	ν_3	2,262	742.6	59.6	0.4	92%S_4 (NNN antisym. str.)
	ν_4	1,667	193.9	192.5	0.2	75%S_5(C=C str.),13%S_8 (CH$_2$ deform.)
	ν_5	1,419	49.1	111.4	0.3	66%S_8 (CH$_2$ deform.), 15%S_7 (NNN sym. str.), 14%S_6 (C–N str.)
	ν_6	1,362	102.8	21.0	0.3	53%S_7 (NNN sym. str.), 21%S_8 (CH$_2$ deform.),11%S_6 (C–N str.)
	ν_7	1,142	104.8	5.1	0.5	52%S_9 (CH$_2$ wag), 18%S_{12} (C=C–N in-plane bend) 13%S_6 (C–N str.)
	ν_8	895	34.2	3.2	0.6	42%S_6 (C–N str.), 36%S_9 (CH$_2$ wag), 12%S_7 (NNN sym. str.)
	ν_9	664	13.6	9.3	0.6	43%S_{11} (NNN in-plane bend), 36%S_{13} (CNN in-plane bend)
	ν_{10}	631	27.7	18.8	0.1	67%S_3 (C$_2$–Cl$_8$ str.)
	ν_{11}	401	1.6	9.8	0.7	36%S_{12} (C=C–N in-plane bend), 27%S_{11} (NNN in-plane bend), 17%S_3 (C$_2$–Cl$_8$ str.), 13%S_{10}(C$_2$–Cl$_8$ in-plane bend)
	ν_{12}	380	1.5	2.3	0.6	58%S_{10} (C$_2$–Cl$_8$ in-plane bend), 26%S_{12} (C=C–N in-plane bend)
	ν_{13}	156	0.1	5.6	0.6	54%S_{13} (CNN in-plane bend), 21%S_{11} (NNN in-plane bend) 15%S_{10} (C$_2$–Cl$_8$ in-plane bend), 11%S_{12} (C=C–N in-plane bend)
A"	ν_{14}	867	59.3	7.2	0.8	99%S_{15} (CH$_2$ deform. I)
	ν_{15}	692	0.2	0.6	0.8	65%S_{16} (CH$_2$ deform. II), 34%S_{14} (C$_2$–Cl$_8$ out-of-plane bend)
	ν_{16}	534	6.7	2.0	0.8	58%S_{14}(C$_2$–Cl$_8$ out-of-plane bend), 26%S_{16} (CH$_2$ deform. II)
	ν_{17}	483	1.8	0.1	0.8	73%S_{17} (NNN wag), 23%S_{16} (CH$_2$ deform. II)
	ν_{18}	65	1.4	0.1	0.8	100%S_{18} (NNN asym. torsion)

[a] IR intensities and Raman activities are calculated in km mol^{-1} and Å^4 amu^{-1} respectively

Table 11 Calculated vibrational frequencies (cm^{-1}) at B3LYP/6-311++G** level for the *cis* conformer of 1-bromovinyl azide

Sym.	No.	Freq.	IR int.[a]	Raman activity	Depol. ratio	PED
A'	ν_1	3,259	0.5	60.4	0.6	92%S_1 (CH$_2$ antisym. str.)
	ν_2	3,152	3.7	88.4	0.1	92%S_2 (CH$_2$ sym. str.)
	ν_3	2,250	537.6	58.0	0.4	91%S_4 (NNN antisym. str.)
	ν_4	1,641	106.4	80.6	0.1	74%S_5 (C=C str.), 16%S_8 (CH$_2$ deform.)
	ν_5	1,424	24.3	42.4	0.2	79%S_8 (CH$_2$ deform.)
	ν_6	1,317	267.8	32.7	0.4	62%S_7 (NNN sym. str.), 16%S_6 (C-N str.)
	ν_7	1,129	118.7	2.2	0.7	56%S_9 (CH$_2$ wag), 11%S_7 (NNN sym. str.), 11%S_{12} (C=C-N in-plane bend)
	ν_8	910	17.9	8.5	0.6	51%S_6 (C-N str.), 19%S_9 (CH$_2$ wag), 11%S_7 (NNN sym. str.)
	ν_9	742	78.4	2.1	0.2	33%S_{13} (CNN in-plane bend), 20%S_{11} (NNN in-plane bend), 18%S_3 (C$_2$-X$_8$ str.), 17%S_9 (CH$_2$ wag), 11%S_{12} (C=C-N in-plane bend)
A''	ν_{10}	543	9.4	7.6	0.1	46%S_{11} (NNN in-plane bend), 23%S_3 (C$_2$-Br$_8$ str.), 16%S_2 (CH$_2$ sym. str.)
	ν_{11}	361	0.8	3.4	0.3	39%S_3 (C$_2$-Br$_8$ str.), 23%S_{10} (C$_2$-Br$_8$ in-plane bend) 34%S_{12} (C=C-N in-plane bend),
	ν_{12}	278	1.0	5.6	0.5	57%S_{10} (C$_2$-Br$_8$ in-plane bend), 15%S_3 (C$_2$-Br$_8$ str.), 11%S_{13} (CNN in-plane bend),
	ν_{13}	156	0.6	8.6	0.5	51%S_{13} (CNN in-plane bend), 23%S_{11} (NNN in-plane bend), 18%S_{12} (C=C-N in-plane bend)
	ν_{14}	852	57.7	3.1	0.8	99%S_{15} (CH$_2$ deform. I)
	ν_{15}	678	0.2	0.2	0.8	78%S_{16} (CH$_2$ deform. II), 22%S_{14} (C$_2$-Br$_8$ out-of-plane bend)
	ν_{16}	525	8.7	0.9	0.8	98%S_{17} (NNN wag)
	ν_{17}	495	2.2	0.8	0.8	76%S_{14} (C$_2$-Br$_8$ out-of-plane bend), 22%S_{16} (CH$_2$ deform. II)
	ν_{18}	62	0.1	3.0	0.8	98%S_{18} (NNN asym. torsion)

[a] IR intensities and Raman activities are calculated in km mol^{-1} and Å^4 amu^{-1} respectively

Table 12 Calculated vibrational frequencies (cm^{-1}) at B3LYP/6-311++G** level for the *trans* conformer of 1-bromovinyl azide

Sym.	No.	Freq.	IR int.[a]	Raman activity	Depol. ratio	PED
A'	ν_1	3,273	0.9	73.8	0.7	96%S_1 (CH$_2$ antisym. str.)
	ν_2	3,166	3.7	140.3	0.2	95%S_2 (CH$_2$ sym. str.)
	ν_3	2,262	725.1	57.4	0.4	92%S_4 (NNN antisym. str.)
	ν_4	1,658	175.9	173.4	0.2	77%S_5 (C=C str.), 13%S_8 (CH$_2$ deform.)
	ν_5	1,420	48.9	110.3	0.3	64%S_8 (CH$_2$ deform.), 16%S_7 (NNN sym. str.), 15%S_6 (C-N str.)
	ν_6	1,364	99.4	18.6	0.3	52%S_7 (NNN sym. str.), 23%S_8 (CH$_2$ deform.), 11%S_6 (C-N str.)
	ν_7	1,129	112.0	7.8	0.3	55%S_9 (CH$_2$ wag), 21%S_{12} (C=C-N in-plane bend), 14%S_6 (C-N str.)
	ν_8	890	36.6	3.1	0.6	45%S_6 (C-N str.), 34%S_9 (CH$_2$ wag), 12%S_7 (NNN sym. str.),
	ν_9	653	11.7	10.6	0.5	44%S_{11} (NNN in-plane bend), 37%S_{13} (CNN in-plane bend)
	ν_{10}	555	20.5	20.9	0.1	50%S_3 (C$_2$-Br$_8$ str.), 26%S_{12} (C=C-N in-plane bend)
	ν_{11}	350	2.7	5.7	0.6	46%S_{10} (C$_2$-Br$_8$ in-plane bend), 30%S_{11} (NNN in-plane bend), 13%S_3 (C$_2$-Br$_8$ str.)
	ν_{12}	338	0.8	7.5	0.6	42%S_{12} (C=C-N in-plane bend), 33%S_3 (C$_2$-Br$_8$ str.), 19%S_{10} (C$_2$-Br$_8$ in-plane bend),
	ν_{13}	133	0.1	6.5	0.6	54%S_{13} (CNN in-plane bend), 27%S_{10} (C$_2$-X$_8$ in-plane bend), 14%S_{11} (NNN in-plane bend)
A''	ν_{14}	870	59.0	5.9	0.8	100%S_{15} (CH$_2$ deform. I)
	ν_{15}	690	0.0	0.9	0.8	71%S_{16} (CH$_2$ deform. II), 26%S_{14} (C$_2$-Br$_8$ out-of-plane bend)
	ν_{16}	509	8.2	1.8	0.8	56%S_{17} (NNN wag), 44%S_{14} (C$_2$-Br$_8$ out-of-plane bend)
	ν_{17}	466	0.2	0.4	0.8	42%S_{17} (NNN wag), 30%S_{16} (CH$_2$ deform. II), 28%S_{14} (C$_2$-Br$_8$ out-of-plane bend)
	ν_{18}	59	1.3	0.2	0.8	100%S_{18} (NNN asym. torsion)

[a] IR intensities and Raman activities are calculated in km mol^{-1} and Å^4 amu^{-1} respectively
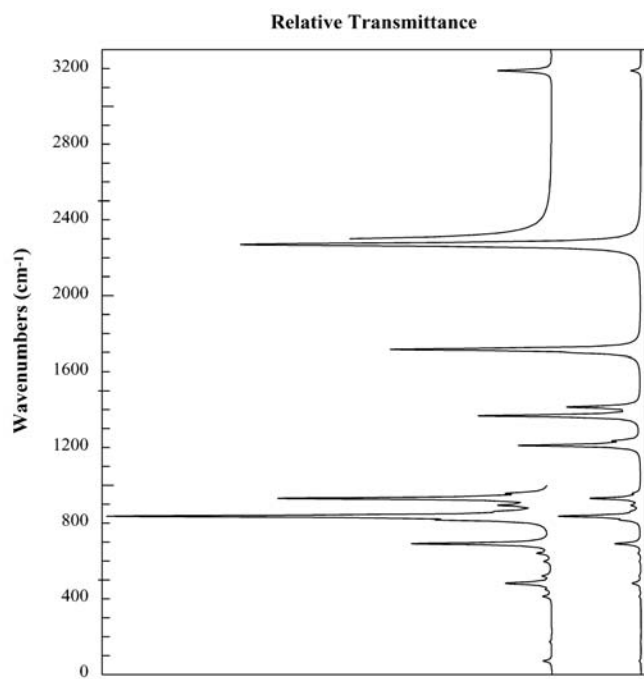
Fig. 3 Calculated vibrational infrared spectrum of 1-fluorovinyl azide at 300 K at the DFT-B3LYP/6-311++G** level
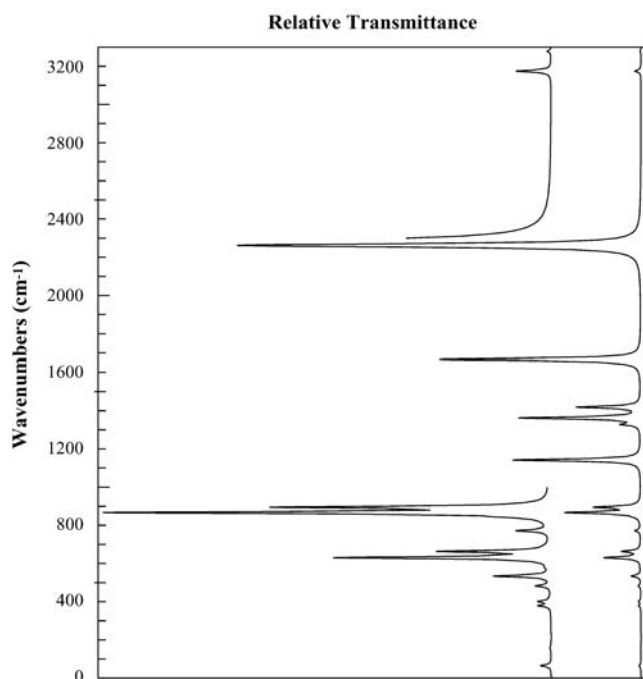

Fig. 5 Calculated vibrational infrared spectrum of 1-chlorovinyl azide at 300 K at the DFT-B3LYP/6-311++G** level
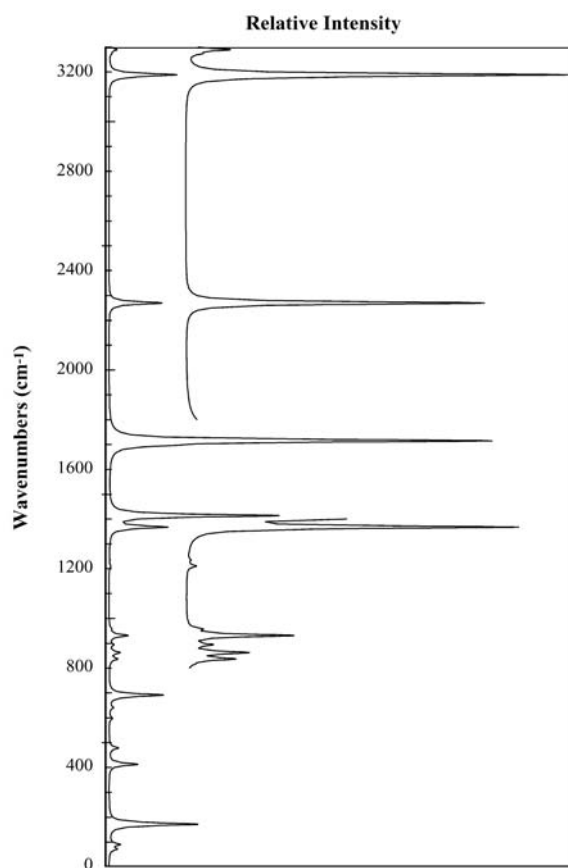

Fig. 4 Calculated vibrational Raman spectrum of 1-fluorovinyl azide at 300 K at the DFT-B3LYP/6-311++G** level
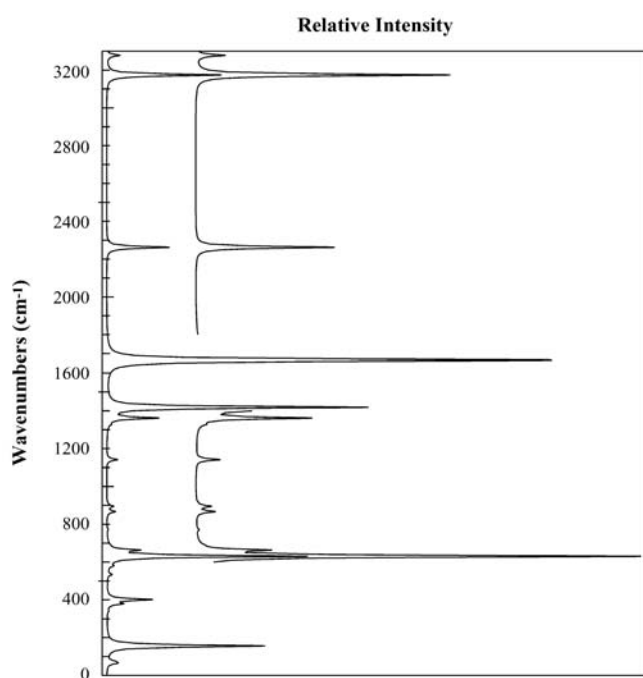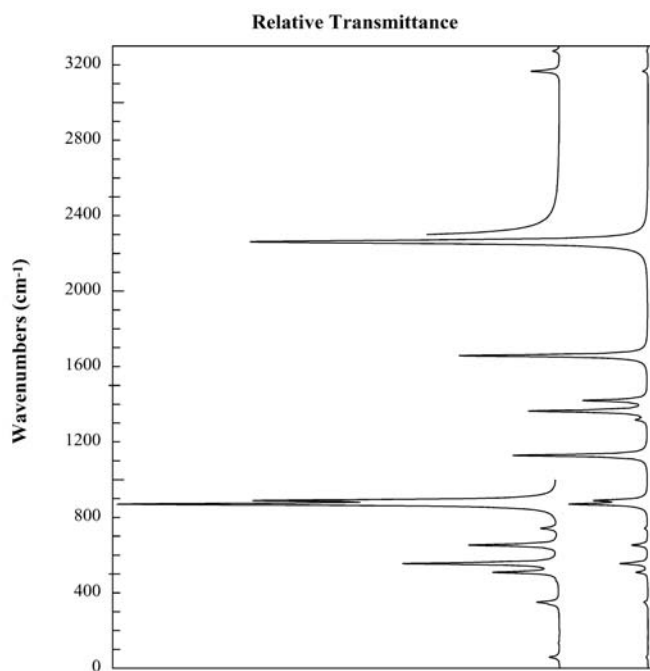

Fig. 6 Calculated vibrational Raman spectrum of 1-chlorovinyl azide at 300 K at the DFT-B3LYP/6-311++G** level

azide mixture (13.5% *cis* and 86.5% *trans*), 1-chlorovinyl azide mixture (4.4% *cis* and 95.6% *trans*) and 1-bromovinyl azide mixture (2.6% *cis* and 97.4% *trans*) are shown in Figs. 3, 4, 5, 6, 7 and 8.

Fig. 7 Calculated vibrational infrared spectrum of 1-bromovinyl azide at 300 K at the DFT-B3LYP/6-311++G** level
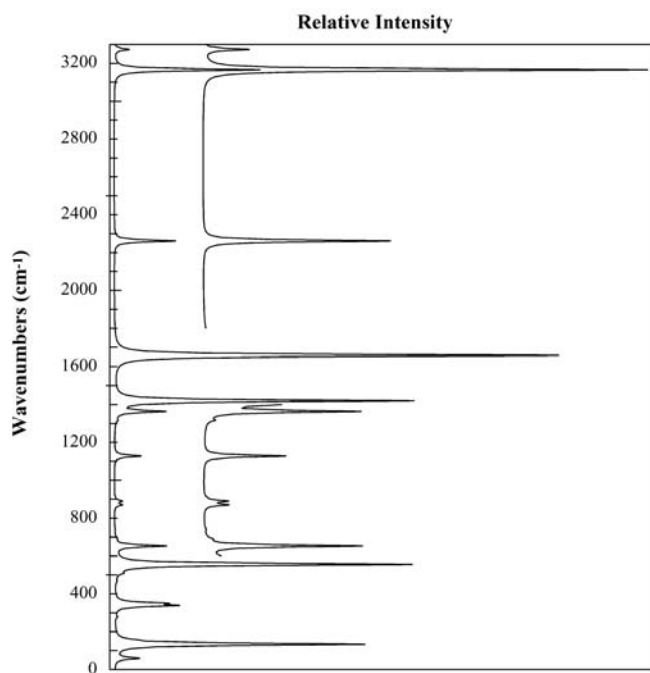
Fig. 8 Calculated vibrational Raman spectrum of 1-bromovinyl azide at 300 K at the DFT-B3LYP/6-311++G** level

Discussion

The high reactivity and importance of organoazides in synthetic chemistry and their applications in many important industries [9, 10, 11, 12, 13, 14, 15, 16, 17, 18, 19, 20, 21, 22, 23, 24] attracted our attention to investigate the structure and conformational behavior of vinyl azide in an earlier study [2] and 1-halovinyl azides $CH_2=CX–NNN$ (where X is fluoro, chloro and bromo) by DFT-B3LYP and ab initio MP2 calculations in the present work.

From full energy optimization, the *trans* conformer was predicted to be the predominant form of the three molecules. Additionally, the relative energy between *cis* and *trans* were calculated at the DFT-B3LYP level to decrease in the order: bromide>chloride>fluoride (2.17 kcal mol^{-1}, 1.82 kcal mol^{-1} and 1.03 kcal mol^{-1}), respectively. The increase in the steric hindrance with the increase in the size of the halogen atom significantly destabilized the *trans* conformation on going from the fluoride, the chloride to the bromide (Fig. 2). This conclusion is supported by the significant change in several structural parameters and the total dipole moment with the change in conformation as going from *cis* to *trans* forms of the molecules (Tables 1 and 2).

The vibrational wavenumbers of 1-fluoro-, 1-chloro- and 1-bromovinyl azides in the *cis* and the *trans* conformations were calculated and the vibrational infrared and Raman spectra were plotted in Figs. 3, 4, 5, 6, 7 and 8. The vibrational assignments of most of the fundamental vibrations of the three molecules were straightforward based on the calculated PED, as given in Tables 7, 8, 9, 10, 11, 12. Since the *trans* is predominantly the low energy conformer of the three molecules, the following discussion will concentrate on the analysis of the vibrational spectra of this conformation (Tables 8, 10 and 12).

The two CH_2 stretching modes (S_1 and S_2) of the vinyl group with the highest wavenumbers in the spectra of the three 1-halovinylazides were predicted to have little mixing with other vibrations (Tables 7, 8, 9, 10, 11, 12). The C=C stretching mode was calculated at about 1,715 cm^{-1} (74% S_5), 1,667 cm^{-1} (75% S_5) and 1,658 cm^{-1} (77% S_5) for the fluoride, the chloride and the bromide as shown in Tables 8, 10 and 12, respectively. This mode was observed at 1,630 cm^{-1} in the Raman spectrum of the *trans* conformation of propenoyl fluoride. [25]

The C–N, C–X and the symmetric NNN stretching modes in the spectra of the molecules were predicted to have a high degree of mixing with other vibrations. However, the antisymmetric NNN stretch was assigned with confidence to the calculated wavenumbers with the highest infrared intensity and negligible mixing at 2,270 cm^{-1} in the spectrum of the fluoride (Table 8) and at 2,262 cm^{-1} in the spectra of the chloride (Table 10) and the bromide (Table 12).

In the case of the bending modes, many were predicted to mix highly with other modes and therefore we could not make conclusive assignments for them based on PED values only. The lowest vibrational torsional mode in the spectra of 1-fluoro-, 1-chloro- and 1-bromovinyl azides were calculated at 72 cm^{-1} (100% PED), 65 cm^{-1} (100%

PED) and 62 cm^{-1} (98% PED), respectively, as shown in Tables 8, 10 and 12.

References

1. Badawi HM, Forner W, Al-Saadi A (2001) J Mol Struct (Theochem) 535:183–197
2. Badawi HM, (2002) J Mol Struct (Theochem) 579:11–19
3. Badawi HM, (2002) J Mol Struct (Theochem) 584:201–210
4. Ford RG (1977) J Mol Spectrosc 65:273–279
5. Frisch MJ, Trucks GW, Schlegel HB, Scuseria GE, Robb MA, Cheeseman JR, Zakrzewski VG, Montgomery JA, Stratman RE, Burant JC, Dapprich S, Millam JM, Daniels AD, Kudin KN, Strain MC, Farkas O, Tomasi J, Barone V, Cossi M, Cammi R, Mennucci B, Pomelli C, Adamo C, Clifford S, Ochterski J, Petersson GA, Ayala PY, Cui Q, Morokuma K, Malick DK, Rabuck AD, Raghavachari K, Foresman JB, Cioslowski J, Ortiz JV, Baboul AG, Stefanov BB, Liu C, Liashenko A, Piskorz P, Komaromi, I, Gomperts R, Martin RL, Fox DJ, Keith T, Al-Laham MA, Peng CY, Nanayakkara A, Gonzalez C, Challacombe M, Gill PMW, Johnson BG, Chen W, Wong MW, Andres JL, Gonzales C, Head-Gordon M, Replogle ES, Pople JA (1998) Gaussian 98. Gaussian, Pittsburgh, Pa.
6. Wilson EB, Decius JC, Cross PC (1995) Molecular vibrations. McGraw-Hill, New York
7. Chantry GW (1997) In: Anderson A (ed) The Raman effect, vol 1. Marcel Dekker, New York, chapter 2
8. Forner W, Badawi HM (2001) J Mol Model 7:288–305
9. Hassner A, Stern M (1986) Angew Chem Int Ed Engl 25:478–479
10. Yu KL, Johnson RL (1987) J Org Chem 52:2051–2059
11. Scriven EFV, Turnabull K (1988) Chem Rev 88:297–368
12. Lowe-Ma CK, Nissan RA, Wilson WS (1990) J Org Chem 55:3755–3761
13. Kamiya N, Shiro Y, Iwata T, Iizulka T, Iwasaki H (1991) J Am Chem Soc 113:1826–1829
14. Aube J, Milligan GL (1991) J Am Chem Soc 113:8965–8966
15. Norris P, Horton D, Levine BR (1995) Tetrahedron Lett 36:7811–7814
16. Milligan GL, Mossman CJ, Aube J (1995) J Am Chem Soc 117:10449–10459
17. Haist R, Mack HG, Vedova COD, Cutin EH, Oberhammer H (1998) J Mol Struct 445:197–205
18. Dyke JM, Groves AP, Morris A, Ogden JS (1999) J Phys Chem A 103:8239–8245
19. Rauhut G, Eckert F (1999) J Phys Chem A 103:9086–9092
20. McIntosch MB, Hartle TJ, Allcock HR (1999) J Am Chem Soc 121:884–885
21. McClelland RA, Ahmed A, Dicks AP, Licence VE (1999) J Am Chem Soc 121:3303–3310
22. Chahona L, Cai H, Fishbein JC (1999) J Am Chem Soc 121:5161–5169
23. Varotsis C, Vamvouka M (1999) J Phys Chem B 103:3942–3946
24. Li L, Wang C, Long Z, FU S (2000) J Polym Sci Part A Polym Chem 38:4519–4523
25. Durig JR, Berry RJ, Groner P (1987) J Chem Phys 87:6303–6322